Received 25 April 2022; accepted 25 July 2022. Date of current version 9 August 2022.
The review of this article was arranged by Editor A. G. U. Perera.

Digital Object Identifier 10.1109/JEDS.2022.3194921

Improved Electrical and Temporal Stability of In-Zn Oxide Semiconductor Thin-Film Transistors With Organic Passivation Layer

KWAN-JUN HEO[1], GERGELY TARSOLY[2], JAE-YUN LEE[2], SEONG GON CHOI[2], JUNG-HYUK KOH[3], AND SUNG-JIN KIM[2]

1 Research and Development Center, SK Hynix, Icheon 13558, Gyeonggi, South Korea
2 College of Electrical and Computer Engineering, Chungbuk National University, Cheongju 28644, South Korea
3 College of Electrical and Electronics Engineering, Chung-Ang University, Seoul 06974, South Korea

CORRESPONDING AUTHOR: S.-J. KIM (e-mail: ksj@cbnu.ac.kr)

This work was supported in part by the Ministry of Science and ICT (MSIT), South Korea, under the Grand Information Technology Research Center Support Program supervised by the Institute for Information and Communications Technology Planning and Evaluation (IITP) under Grant IITP-2020-0-01462, and in part by the Basic Science Research Program through the National Research Foundation of Korea (NRF) funded by the Ministry of Education under Grant 2020R1A6A1A12047945.

ABSTRACT Solution-processed In-Zn oxide (IZO) semiconductor thin-film transistors (TFTs) were fabricated with passivation layers of either poly(methyl methacrylate) (PMMA) or cyclic transparent optical polymer (CYTOP). According to the transfer curves obtained on the day of fabrication and after 200 days, the drain-source current of the IZO TFT without a passivation layer decreased by approximately 37 %. For the PMMA-passivated IZO TFT, it decreased by approximately 31 %. The current for the CYTOP-passivated IZO TFT showed significantly lower, only 7 % deterioration. Hence, the CYTOP-passivated IZO TFT exhibited improved electrical stability under long term ambient storage. This was attributed to the difference in the chemical composition of the two polymers, as CYTOP is a fluoropolymer, while PMMA is an ester group containing organic polymer. We show, passivation of the active layer with the proper organic film improves the stability of the high-performance solution-processed IZO TFTs.

INDEX TERMS IZO, oxides semiconductor, passivation, thin-film transistor.

I. INTRODUCTION

Amorphous oxide semiconductor thin-film transistors (TFTs) have attracted interest for use in modern electronics owing to their high electron mobility and stability [1]–[5]. Among them, indium–zinc oxide (IZO) is attracting attention as a promising candidate for next-generation display backplanes owing to its uniformity in large-area thin films, excellent transmittance in the visible region (∼90 %), and relatively high electron mobility (∼10 cm^2/Vs) compared to commercial amorphous or poly-Si-based semiconductors [6], [7].

Although IZO TFTs have excellent electrical characteristics, the device properties may deteriorate over time owing to instability under ambient conditions [8], [9]. In IZO, the ionic character of the bonds between atoms are stronger than the van der Waals interaction in molecular semiconductors [10], [11], but the binding energies are low compared to those with covalent bonds. Therefore the IZO is susceptible to surface defects such as interstitial defects, oxygen vacancies, and doping by unspecified molecules from the environment [6], [12]. The surface of the oxide might also promote redox reactions with gases adsorbed from the surrounding ambient air [13], [14]. Furthermore, when materials with ionic bonds are exposed to light, the low binding energy might promote defect formation, consequently, exposure to light can degrade the TFT performance [15].

To address these stability problems, it is essential to form a passivation layer on the oxide surface. This layer can protect the oxide semiconductor from the penetration of oxygen and moisture from the environment, thereby preventing undesirable oxidation/reduction reactions [2], [16]–[18]. Recent studies have also shown that a passivation layer improves the electrical properties of TFTs by reducing the uncoordinated oxygen species [2] at the channel interface [19].

This work is licensed under a Creative Commons Attribution 4.0 License. For more information, see https://creativecommons.org/licenses/by/4.0/

 JOURNAL OF THE ELECTRON DEVICES SOCIETY

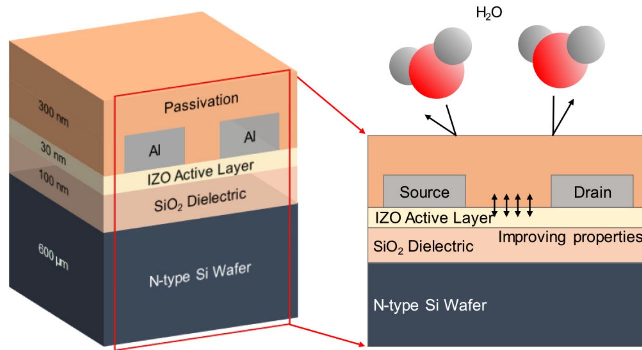

FIGURE 1. Schematic diagram of the structure of IZO/SiO_2 TFT with a passivation layer that protects the active layer surface from the ambient environment.

To improve the electrical characteristics and long-term stability of the solution-processed IZO TFTs, a passivation strategy is proposed, in which polymers with low reactivity and hydrophobic properties are used as the passivation layer. Increased stability and improvement of electrical characteristics of metal oxide semiconductors such as indium gallium zinc oxide has been described in the literature when using cyclic transparent optical polymer (CYTOP) [17], [20] or poly(methyl methacrylate) (PMMA) [21] passivation layers. Therefore, in our study, PMMA was selected as a representative non-fluorinated polymer as it has been successfully employed as a component in a multi-layer passivation film over solution-processed IZO for fabricating water-proof electronics [22]. However, long-term stability assessment was not carried out. Several fluorinated polymers have been in use in electronic devices because of the polarity of the C-F bonds [23]. As a representative fluorinated polymer, CYTOP was selected due to its versatility [24] and its successful application as passivation layer for a complementary circuit with IZO and an organic semiconductor [25]. Moreover, these materials have also been applied experimentally as a passivation layer in organic semiconductors where preventing the performance degradation due to the environment is extremely important due to the higher degradation when compared to inorganic semiconductors, which prove their effectiveness [6], [26].

In this study, the practical applicability of PMMA- and CYTOP-based passivation layers in the IZO TFTs was analyzed by comparing the effect of the polymers on TFT performance and bias stability. Finally, the changes in the I-V characteristics over long-term storage were observed to examine the effects of each type of passivation layer on the performance of the IZO TFT and in comparision to the TFT with unprotected IZO after 200 days.

II. EXPERIMENTS SETTING

Fig. 1 presents a schematic diagram of the IZO/silicon dioxide (SiO_2) TFT fabricated in this study, which has a top-contact, bottom-gate structure, and demonstrates the effects of the passivation layer by protecting the metal oxide from ambient water vapor. An IZO TFT with a Si substrate (600 μm)/SiO_2 (100 nm)/IZO (30 nm)/Al (100 nm)/PMMA or CYTOP (300 nm) structure was fabricated. A heavily doped n-type Si wafer, approximately 600 μm in thickness, was used as the substrate and gate electrode. To form the dielectric layer, an approximately 100 nm thick SiO_2 thin film was grown in a furnace. To remove surface defects (metallic defects and organic particles), a 4:1 volume ratio mixture of sulfuric acid (H_2SO_4) and hydrogen peroxide (H_2O_2) were used to clean the surface for approximately 60 min at 90 °C.

Indium nitrate hydrate [$In(NO_3)_3{\cdot}9H_2O$] and zinc acetate dihydrate [$Zn(CH_3COO)_2{\cdot}2H_2O$] were used as solutes to form a solution-processed IZO active layer, and 2-methoxyethanol was used as a solvent to prepare 0.1 M solutions with respect to In and Zn content. Acetylacetone was added to the solution to serve as combustible material, aiding the conversion of the precursors to metal oxide; ammonia (NH_3) was added to the In precursor solution as a chelating agent [27], [28]. The solutions were then stirred for approximately 2 h at 60 °C in a water bath to maintain a constant temperature. The In and Zn solutions were then mixed at a 7:3 ratio and stirred for approximately 2 h at 27 °C. Subsequently, the IZO solution was spin-coated on top of the SiO_2 at 1,500 rpm to fabricate an IZO semiconductor active layer with a thickness between 20 to 30 nm. To evaporate the remaining solvent, the film was annealed at 400 °C for approximately 4 h using a hotplate. A 100-nm-thick Al source-drain electrode was deposited on top of the IZO active layer using a thermal evaporator to form a channel layer, 200 μm in length and 2,000 μm in width.

Finally, to form the protective film, PMMA and CYTOP were dissolved separately in toluene and spin-coated onto an IZO TFT at 2,500 rpm for approximately 40 s. The film was then heat-treated for 2 h at 100 °C in a vacuum oven to form a PMMA or CYTOP passivation layer. The electrical characteristics of the three types of IZO TFTs [with a PMMA passivation layer (PP), with a CYTOP passivation layer (CP), and without a passivation layer (WOP)] were examined using a semiconductor analyzer (Agilent 1500B) to measure the I-V curves at room temperature. The bias stability of the devices was measured by recording the I-V curves after applying bias stress to the gate electrode. Furthermore, the I-V measurements of the as-fabricated TFT ("pristine") and the TFT after 200 days were compared to investigate the passivation effect over time.

III. RESULTS AND DISCUSSION

In Fig. 2, we show the measured electrical characteristics of the PP, CP, and WOP IZO TFTs, which demonstrate the effect of the passivation layer on the performance of the IZO TFTs. Fig. 2(a) presents the output curve [drain-source current (I_{ds}) *vs* the drain-source voltage (V_{ds}) at different constant gate voltages (V_{gs})] of the devices. The pristine *I–V* curves of the three types of TFT were similar, whereas the measurements after 200 days showed the effects of the

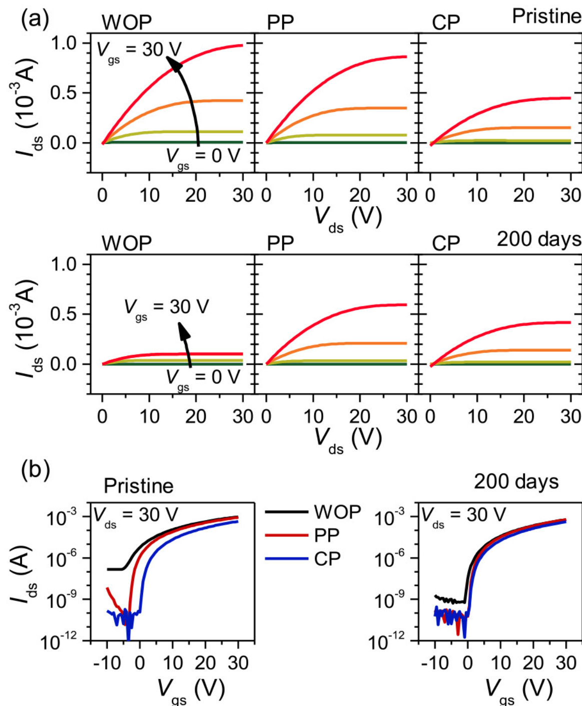

FIGURE 2. (a) Output curves at $V_{gs} = 0, 10, 20$ and 30 V, (b) transfer curves at $V_{ds} = 30$ V of the WOP, PP, and CP TFTs in the pristine state and after 200 days.

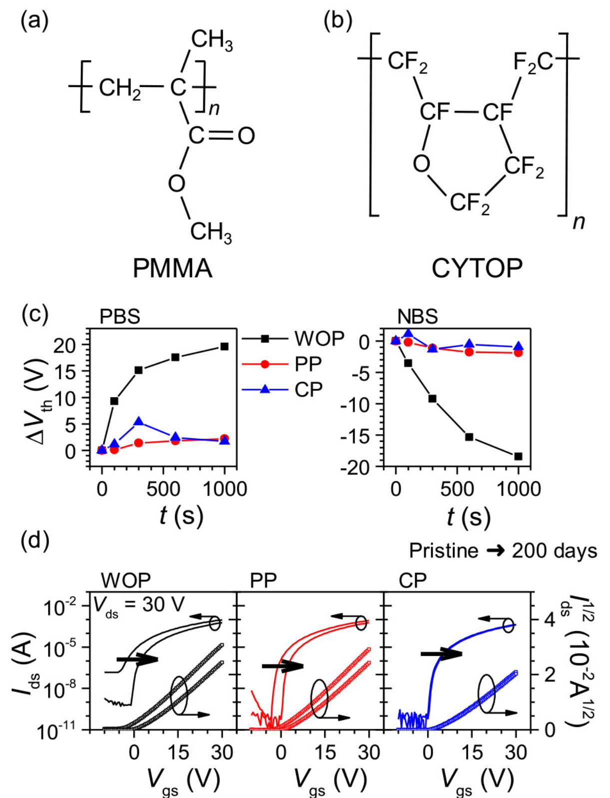

FIGURE 3. Chemical structures of (a) PMMA and (b) CYTOP, (c) threshold voltage shift during positive bias stress (PBS) and negative bias stress (NBS), and (d) transfer curves at $V_{ds} = 30$ V of the WOP, PP, and CP TFTs in the pristine state and after 200 days.

passivation layer. The pristine output curve of all the devices showed similar characteristics. The WOP IZO TFT shows both the highest off current and on current, which is interpreted as an increase due to the unintentional doping of unspecified molecules because the IZO active layer was exposed to the environment [29], [30]. The highest currents of the pristine samples in the saturation state were approximately 9.8×10^{-4}, 8.6×10^{-4}, and 4.5×10^{-4} A for the WOP, PP, and CP IZO TFTs, respectively. After 200 days, the highest currents were 1.0×10^{-4}, 5.9×10^{-4}, and 4.2×10^{-4} A, respectively. The current of the WOP, PP, and CP TFTs decreased by approximately 90 %, 31 %, and 6 %, respectively, after 200 days compared to the pristine sample. This shows that the I-V characteristics of the IZO TFTs with a passivation layer exhibited relatively small changes.

Fig. 2(b) shows the transfer curve (I_{ds} vs V_{gs}) at $V_{ds} = 30$ V, where V_{gs} was swept from -10 to 30 V in 0.2 V steps. Interestingly, the off-current level of the WOP IZO TFT improved after 200 days, which might be caused by several factors in the device that was not protected from the environment, such as removal of residual solvent, changing contamination profile or changing crystallinity [31]. On the other hand, the threshold voltage (V_{th}) shifted slightly [32], [33]. In contrast, the off currents of the IZO TFTs with a passivation layer varied within approximately 10 %. This is because the passivation layer physically limits deterioration by limiting the adsorption of oxygen and moisture on the back of the IZO active layer [18], [34]. Hence, it blocks the leakage current caused by interfacial defects. In addition, as the active layer was not patterned, parasitic current paths can form at the corner or edge of the patterned source / drain electrodes. However, the passivation layer acts as an insulating dielectric layer, which might reduce the leakage current by removing the parasitic current paths at the edges.

Fig. 3(a) shows the chemical structure of the PMMA and Fig. 3(b) shows that of CYTOP. The chemical and physical characteristics of the PMMA are dominated by relatively short, non-polar C-H single covalent bonds with a binding energy of approximately 410 kJ/mol, which are relatively non-polar [35], [36]. However, the C = O groups in the ester bond of the PMMA give the molecule a somewhat polar character, resulting in a dielectric constant measured around 2.6∼3.0 [37], [38]. The CYTOP on the other hand is characterized by C-F bonds that are also short single bonds, and they become shorter and stronger as the fluorine content increases [23]. In CYTOP, which contains no H, C-F bonds have a binding energy of approximately 450 kJ/mol. These bonds are more polar than the C-H bonds of the PMMA. On the other hand, the C-O-C found in CYTOP is the most non-polar of the C-O bonds, resulting in a dielectric constant of around 2 for the CYTOP [17], [39], [40]. To compare the hydrophilic properties of the bare IZO and the passivation layers, the contact angle of a water droplet was measured on IZO, PMMA covered IZO and CYTOP covered IZO. It was found that the contact angle of the IZO is 52°, which

TABLE 1. Electrical parameters of IZO/SiO_2 TFTs using WOP, PP, and CP layers in the pristine state and after 200 days, and tolerance.

Sample	Time	μ_{sat} (cm^2/Vs)	On/off current ratio	V_{th} (V)	S/S (V/dec)
WOP	Pristine	6.3	6.5×10^3	0.2	2.6
	200 days	5.6	1.1×10^6	5.1	0.7
	Tolerance (delta)	±0.4	$\pm 5.5 \times 10^3$	±2.5	±1.0
PP	Pristine	6.5	1.4×10^8	2.2	0.5
	200 days	5.8	2.1×10^8	5.7	0.5
	Tolerance (delta)	±0.4	$\pm 0.4 \times 10^8$	±1.8	-
CP	Pristine	6.5	7.6×10^8	5.3	0.4
	200 days	6.5	2.3×10^8	5.9	0.5
	Tolerance (delta)	-	$\pm 2.7 \times 10^8$	±0.3	±0.1

shows moderate hydrophilicity due to the OH groups at the oxide surface and might strongly interact with water from the atmosphere. The water contact angle is 75° for PMMA and 106° for CYTOP, which show strong hydrophobicity, especially for the fluoropolymer.

It has been previously shown that under high temperatures (350 °C), F atoms can be cleaved from the polymer, and diffuse into metal oxides, however at the processing temperatures used in this study for the deposition of CYTOP, that effect is not significant [20].

The bias stress stability of three device types was assessed under $V_{gs} = 20$ V for the PBS and under $V_{gs} = -20$ V for the NBS measurements, and the shift in threshold voltage (ΔV_{th}) is plotted on Fig. 3(c). Based on the transfer curves measured before and multiple times during the bias stress up to 1000 s, it was found, that for the WOP devices V_{th} has changed significantly even after a 100 s. After 1000 s, ΔV_{th} was 20 V under positive bias stress and -18 V under the negative bias stress. However, for the passivated devices, the ΔV_{th} after 1000 s was less than 3 V for PBS and less than -2 V for NBS, for both PP and CP devices.

Fig. 3(d) shows the changes in the transfer curves of the WOP, PP, and CP IZO TFTs over time. At $V_{ds} = 30$ V, the I_{ds} value of the WOP IZO TFT decreased by approximately 37 %. In contrast, the I_{ds} value of the PP IZO TFT decreased by approximately 31 %, and the CP IZO TFT exhibited relatively smaller, 7 % deterioration in I_{ds} in the on state. This suggests that the defect density related to charge trapping between the IZO and CYTOP is very small [17]. Moreover, in CYTOP, which has a relatively high binding energy, uncoordinated oxygen species of the semiconducting IZO active layer cannot form covalent bonds with other atoms [41]. The results suggest that CYTOP has superior ability to suppress the formation interfacial defects to that of PMMA.

Fig. 4 presents box plots of the electron mobility, on/off current ratios, and V_{th} of the WOP, PP, and CP IZO TFTs. Table 1 lists the performance parameters. The electrical characteristics of the WOP, PP, and CP IZO TFTs in the pristine state and after 200 days are as follows. The mean electron mobility of the WOP, PP, and CP IZO TFTs diminished

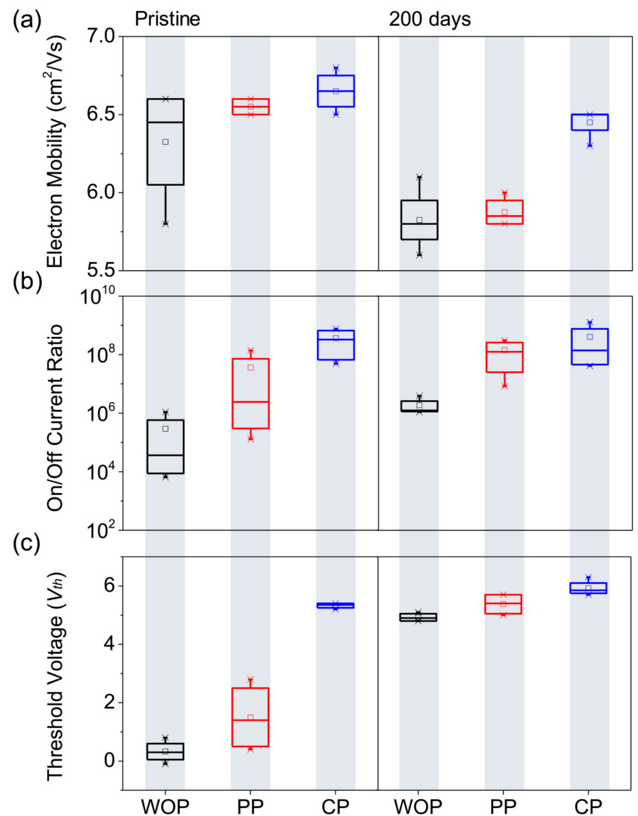

FIGURE 4. Box plots of the electron mobility, on/off current ratio, and V_{th} of the WOP, PP, and CP IZO/SiO_2 TFTs in the pristine state and after 200 days.

by approximately 0.5, 0.7, and 0.2 cm^2/Vs, respectively (Fig. 4 a). Interestingly, the on/off current ratio of the devices WOP and PP increased during the 200 day period, however, at approximately 10^6 for WOP, and 10^8 for PP, the mean on/off current ratio of the CP IZO TFTs is still the highest at 4×10^8 after 200 days (Fig. 4 b). The mean V_{th} of the WOP, PP, and CP IZO TFTs increased by approximately 4.6, 3.9, and 0.6 V, respectively, after 200 days compared to the as-deposited devices (Fig. 4 c). Contrasting the statistical

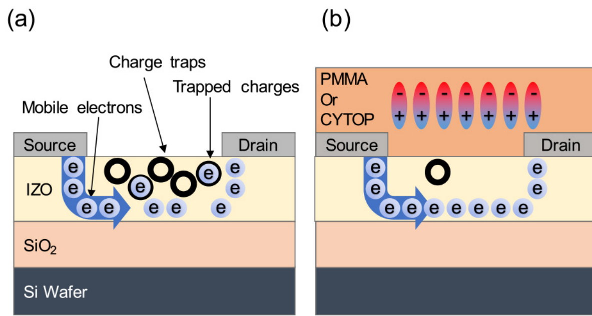

FIGURE 5. Schematic illustrations of (a) WOP, (b) PP, and CP IZO TFT operation under positive gate bias.

distributions of the electrical characteristics of the WOP, PP, and CP IZO TFTs in the pristine state and after 200 days, the rates of changes for the WOP and PP IZO TFTs were relatively high. In contrast, the CP IZO TFT exhibited the lowest rate of change. These results indicate that the device stability was significantly affected by the type of the polymer passivation layer. Owing to the high hydrophobicity as shown by the high water contact angle, the CYTOP fluoropolymer is much more effective in protecting the active layer from ambient moisture than the slightly hydrophilic PMMA [42].

Fig. 5 presents the schematics of the cross-section in the IZO channel region under bias with and without a passivation layer. The cross-section of the WOP IZO TFT in Fig. 5(a) shows that owing to interface defects on the back of the IZO active layer, a relatively large density of trap sites was created, which impedes the charge transport. A cross-section of the passivated IZO TFT in Fig. 5(b) demonstrates the effects of the passivation layer on the channel when positive bias was applied to the gate. PMMA, which contains a carboxyl group, forms a relatively strong dipole, which interacts with the mobile charges in the IZO active layer and might affect the trapping behavior [43]. CYTOP on the other hand, despite the polar C-F bonds, has a lower dielectric constant, and this relatively low polarity results in reduced dipolar disorder at the IZO/CYTOP interface [17], [39]. The disorder and trap site density is reduced by the lack of hydroxyl and amine bonds on the back of the IZO active layer due to the blocking of moisture and other contaminants from the air. The tenfold decrease in threshold voltage shift under bias stress for the passivated devices relative to that of the WOP device can also be attributed to the reduction in trap site density, as the passivation effects aided in improving the reliability and electrical characteristics of the PP and CP devices, compared to those of WOP IZO TFTs [11], [38], [43].

IV. CONCLUSION

In summary, we proposed a solution-processed IZO TFT with two types of polymer passivation layers to improve the electrical characteristics and stability of the device. The *I–V* characteristics were measured in the pristine state and after storage for 200 days, and for comparison, IZO TFT without passivation has also been characterized under the same conditions. The current levels in the on state for WOP, PP, and CP IZO TFTs decreased by approximately 37 %, 31 %, and 7 %, respectively. This shows that the I–V characteristics of the IZO TFTs with a passivation layer deteriorated to a much lower degree when compared to the device without passivation. The statistical distributions of the electron mobility, on/off current ratio, and V_{th}, which indicate the TFT electrical characteristics, were also analyzed and the device with CYTOP passivation showed the best performance stability. These results suggest that the device stability is affected by the material of the passivation layer which is well demonstrated via the difference in stability when using either the slightly hydrophilic PMMA or the strongly hydrophobic CYTOP polymer as passivation layer. The solution-process-based passivation treatment proposed in this study can be used to improve the electrical characteristics and stability of IZO TFTs, which can be applied to the backplane of displays.

REFERENCES

[1] T. S. Jung, H. Lee, H. J. Kim, J. H. Lee, and H. J. Kim, "Dual-functional superoxide precursor to improve the electrical characteristics of oxide thin film transistors," *ACS Appl. Mater. Interfaces*, vol. 10, no. 51, pp. 44554–44560, 2018, doi: 10.1021/acsami.8b16961.
[2] Y. J. Tak *et al.*, "Multifunctional, room-temperature processable, heterogeneous organic passivation layer for oxide semiconductor thin-film transistors," *ACS Appl. Mater. Interfaces*, vol. 12, no. 2, pp. 2615–2624, 2020, doi: 10.1021/acsami.9b16898.
[3] J. H. Lee, S. P. Park, K. Park, and H. J. Kim, "Flexible and waterproof resistive random-access memory based on nitrocellulose for skin-attachable wearable devices," *Adv. Funct. Mater.*, vol. 30, no. 1, 2020, Art. no. 1907437, doi: 10.1002/adfm.201907437.
[4] Y. S. Jung *et al.*, "Balanced performance enhancements of a-InGaZnO thin film transistors by using all-amorphous dielectric multilayers sandwiching high-k CaCu3Ti4O12," *Adv. Electron. Mater.*, vol. 5, no. 10, 2019, Art. no. 1900322, doi: 10.1002/aelm.201900322.
[5] S.-J. Seo, S. Yang, J.-H. Ko, and B.-S. Bae, "Effects of sol-gel organic-inorganic hybrid passivation on stability of solution-processed zinc tin oxide thin film transistors," *Electrochem. Solid-State Lett.*, vol. 14, no. 9, 2011, Art. no. H375, doi: 10.1149/1.3603845.
[6] S. Hu *et al.*, "Effect of Al2O3 passivation layer and cu electrodes on high mobility of amorphous IZO TFT," *IEEE J. Electron Devices Soc.*, vol. 6, pp. 733–737, 2018, doi: 10.1109/JEDS.2018.2820003.
[7] W. Wu *et al.*, "A high-reliability gate driver integrated in flexible AMOLED display by IZO TFTs," *IEEE Trans. Electron Devices*, vol. 64, no. 5, pp. 1991–1996, May 2017, doi: 10.1109/TED.2016.2641448.
[8] N. Tiwari, R. N. Chauhan, P.-T. Liu, and H.-P. D. Shieh, "Modification of intrinsic defects in IZO/IGZO thin films for reliable bilayer thin film transistors," *RSC Adv.*, vol. 6, no. 79, pp. 75693–75698, 2016, doi: 10.1039/C6RA13208A.
[9] Y. Goh *et al.*, "Defects and charge-trapping mechanisms of double-active-layer In–Zn–O and Al–Sn–Zn–In–O thin-film transistors," *ACS Appl. Mater. Interfaces*, vol. 9, no. 11, pp. 9271–9279, 2017, doi: 10.1021/acsami.7b01533.
[10] Y. Lee *et al.*, "Universal oriented van der waals epitaxy of 1d cyanide chains on hexagonal 2D crystals," *Adv. Sci.*, vol. 7, no. 4, 2020, Art. no. 1900757, doi: 10.1002/advs.201900757.
[11] G. Dastgeer *et al.*, "Black phosphorus-IGZO van der waals diode with low-resistivity metal contacts," *ACS Appl. Mater. Interfaces*, vol. 11, no. 11, pp. 10959–10966, 2019, doi: 10.1021/acsami.8b20231.
[12] D. Wan *et al.*, "Design of highly stable tungsten-doped IZO thin-film transistors with enhanced performance," *IEEE Trans. Electron Devices*, vol. 65, no. 3, pp. 1018–1022, Mar. 2018, doi: 10.1109/TED.2018.2797300.

[13] B. S. Shaheen *et al.*, "Real-space mapping of surface-oxygen defect states in photovoltaic materials using low-voltage scanning ultrafast electron microscopy," *ACS Appl. Mater. Interfaces*, vol. 12, no. 6, pp. 7760–7767, 2020, doi: 10.1021/acsami.9b20215.

[14] X. Tao, D. Zhang, W. Ma, X. Liu, and D. Xu, "Automatic metallic surface defect detection and recognition with convolutional neural networks," *Appl. Sci.*, vol. 8, no. 9, p. 1575, 2018, doi: 10.3390/app8091575.

[15] J. Bang, S. Matsuishi, and H. Hosono, "Hydrogen anion and subgap states in amorphous In–Ga–Zn–O thin films for TFT applications," *Appl. Phys. Lett.*, vol. 110, no. 23, 2017, Art. no. 232105, doi: 10.1063/1.4985627.

[16] C. R. Allemang and R. L. Peterson, "Passivation of thin channel zinc tin oxide TFTs using Al2O3 deposited by O3-based atomic layer deposition," *IEEE Electron Device Lett.*, vol. 40, no. 7, pp. 1120–1123, Jul. 2019, doi: 10.1109/LED.2019.2914238.

[17] S.-H. Choi, J.-H. Jang, J.-J. Kim, and M.-K. Han, "Low-temperature organic (CYTOP) passivation for improvement of electric characteristics and reliability in IGZO TFTs," *IEEE Electron Device Lett.*, vol. 33, no. 3, pp. 381–383, Mar. 2012, doi: 10.1109/LED.2011.2178112.

[18] S. Hong, S. P. Park, Y.-G. Kim, B. H. Kang, J. W. Na, and H. J. Kim, "Low-temperature fabrication of an HfO2 passivation layer for amorphous indium–gallium–zinc oxide thin film transistors using a solution process," *Sci. Rep.*, vol. 7, no. 1, 2017, Art. no. 16265, doi: 10.1038/s41598-017-16585-x.

[19] S. Sanctis, R. C. Hoffmann, M. Bruns, and J. J. Schneider, "Direct photopatterning of solution–processed amorphous indium zinc oxide and zinc tin oxide semiconductors—A chimie douce molecular precursor approach to thin film electronic oxides," *Adv. Mater. Interfaces*, vol. 5, no. 15, 2018, Art. no. 1800324, doi: 10.1002/admi.201800324.

[20] K.-M. Jung *et al.*, "Stability improvement of solution-processed IGZO TFTs by fluorine diffusion from a CYTOP passivation layer," *J. Phys. D, Appl. Phys.*, vol. 53, no. 35, 2020, Art. no. 355107, doi: 10.1088/1361-6463/ab8e7d.

[21] D. H. Kim *et al.*, "High stability InGaZnO4 thin-film transistors using sputter-deposited PMMA gate insulators and PMMA passivation layers," *Electrochem. Solid-State Lett.*, vol. 12, no. 8, 2009, Art. no. H296, doi: 10.1149/1.3142470.

[22] X. Wei, S. Kumagai, M. Sasaki, S. Watanabe, and J. Takeya, "Stabilizing solution-processed metal oxide thin-film transistors via trilayer organic–inorganic hybrid passivation," *AIP Adv.*, vol. 11, no. 3, 2021, Art. no. 35027, doi: 10.1063/5.0038128.

[23] A.T. Lill *et al.*, "High-k fluoropolymer gate dielectric in electrically stable organic field-effect transistors," *ACS Appl. Mater. Interfaces*, vol. 11, no. 17, pp. 15821–15828, 2019, doi: 10.1021/acsami.8b20827.

[24] R. Min, B. Ortega, A. Leal-Junior, and C. Marques, "Fabrication and characterization of bragg grating in CYTOP POF at 600-nm wavelength," *IEEE Sens. Lett.*, vol. 2, no. 3, pp. 1–4, Sep. 2018, doi: 10.1109/LSENS.2018.2848542.

[25] M.H. Kang, J. Armitage, Z. Andaji-Garmaroudi, and H. Sirringhaus, "Surface passivation treatment to improve performance and stability of solution-processed metal oxide transistors for hybrid complementary circuits on polymer substrates," *Adv. Sci.*, vol. 8, no. 23, 2021, Art. no. 2101502, doi: 10.1002/advs.202101502.

[26] Y. Xu *et al.*, "Essential effects on the mobility extraction reliability for organic transistors," *Adv. Funct. Mater.*, vol. 28, no. 42, 2018, Art. no. 1803907, doi: 10.1002/adfm.201803907.

[27] J. W. Hennek, M.-G. Kim, M. G. Kanatzidis, A. Facchetti, and T. J. Marks, "Exploratory combustion synthesis: Amorphous indium yttrium oxide for thin-film transistors," *J. Amer. Chem. Soc.*, vol. 134, no. 23, pp. 9593–9596, 2012, doi: 10.1021/ja303589v.

[28] J.W. Hennek *et al.*, "Oxygen 'getter' effects on microstructure and carrier transport in low temperature combustion-processed a-InXZnO (X = Ga, Sc, Y, La) transistors," *J. Amer. Chem. Soc.*, vol. 135, no. 29, pp. 10729–10741, 2013, doi: 10.1021/ja403586x.

[29] D. J. Byun, J. D. Wolchok, L. M. Rosenberg, and M. Girotra, "Cancer immunotherapy—Immune checkpoint blockade and associated endocrinopathies," *Nat. Rev. Endocrinol.*, vol. 13, no. 4, pp. 195–207, 2017, doi: 10.1038/nrendo.2016.205.

[30] S. Hu *et al.*, "High mobility amorphous indium-gallium-zinc-oxide thin-film transistor by aluminum oxide passivation layer," *IEEE Electron Device Lett.*, vol. 38, no. 7, pp. 879–882, Jul. 2017, doi: 10.1109/LED.2017.2702570.

[31] J. Choi *et al.*, "Low-temperature solution-based In_2O_3 channel formation for thin-film transistors using a visible laser-assisted combustion process," *IEEE Electron Device Lett.*, vol. 38, no. 9, pp. 1259–1262, Sep. 2017, doi: 10.1109/LED.2017.2734905.

[32] C. Lin, P. Chen, P. Lai, C. Hsu, and J. Chang, "Amorphous IGZO TFT-based pixel buffer to suppress blue-phase liquid crystal high-frequency effect," *IEEE Electron Device Lett.*, vol. 38, no. 12, pp. 1673–1675, Dec. 2017, doi: 10.1109/LED.2017.2763610.

[33] J. Park, K. S. Jang, D. G. Shin, M. Shin, and J. S. Yi, "Gate-induced drain leakage current characteristics of P-type polycrystalline silicon thin film transistors aged by off-state stress," *Solid-State Electron.*, vol. 148, pp. 20–26, Oct. 2018, doi: 10.1016/j.sse.2018.07.009.

[34] Y. Chien *et al.*, "Role of H_2O molecules in passivation layer of a-InGaZnO thin film transistors," *IEEE Electron Device Lett.*, vol. 38, no. 4, pp. 469–472, Apr. 2017, doi: 10.1109/LED.2017.2666198.

[35] J. Lee *et al.*, "Enhanced electrical stability of organic thin-film transistors with polymer semiconductor-insulator blended active layers," *Appl. Phys. Lett.*, vol. 100, no. 8, 2012, Art. no. 83302, doi: 10.1063/1.3688177.

[36] M. Lily, B. Baidya, and A. K. Chandra, "Theoretical studies on atmospheric chemistry of HFE-245mc and perfluoro-ethyl formate: Reaction with OH radicals, atmospheric fate of alkoxy radical and global warming potential," *Chem. Phys. Lett.*, vol. 669, pp. 211–217, Feb. 2017, doi: 10.1016/j.cplett.2016.12.037.

[37] S. Gross, D. Camozzo, V. Di Noto, L. Armelao, and E. Tondello, "PMMA: A key macromolecular component for dielectric low-κ hybrid inorganic–organic polymer films," *Eur. Polym. J.*, vol. 43, no. 3, pp. 673–696, 2007, doi: 10.1016/j.eurpolymj.2006.12.012.

[38] J. Park *et al.*, "Flexible and transparent organic phototransistors on biodegradable cellulose nanofibrillated fiber substrates," *Adv. Opt. Mater.*, vol. 6, no. 9, 2018, Art. no. 1701140, doi: 10.1002/adom.201701140.

[39] A. S. Safaruddin *et al.*, "Highly reliable low-temperature (180 °C) solution-processed passivation for amorphous In–Zn–O thin-film transistors," *Appl. Phys. Exp.*, vol. 12, no. 6, 2019, Art. no. 64002, doi: 10.7567/1882-0786/ab1726.

[40] Y.-Y. Lin, R. D. Evans, E. Welch, B.-N. Hsu, A. C. Madison, and R. B. Fair, "Low voltage electrowetting-on-dielectric platform using multi-layer insulators," *Sens. Actuators B, Chem.*, vol. 150, no. 1, pp. 465–470, 2010, doi: 10.1016/j.snb.2010.06.059.

[41] A. Liu, H. Zhu, H. Sun, Y. Xu, and Y.-Y. Noh, "Solution processed metal oxide high-k dielectrics for emerging transistors and circuits," *Adv. Mater.*, vol. 30, no. 33, 2018, Art. no. 1706364, doi: 10.1002/adma.201706364.

[42] J. M. Kim, J. Oh, K.-M. Jung, K. Park, J.-H. Jeon, and Y.-S. Kim, "Ultrathin flexible thin film transistors with CYTOP encapsulation by debonding process," *Semicond. Sci. Technol.*, vol. 34, no. 7, 2019, Art. no. 75015, doi: 10.1088/1361-6641/ab2201.

[43] K. C. Kwon, S. Kim, C. Kim, J.-L. Lee, and S. Y. Kim, "Fluoropolymer-assisted graphene electrode for organic light-emitting diodes," *Org. Electron.*, vol. 15, no. 11, pp. 3154–3161, 2014, doi: 10.1016/j.orgel.2014.08.041.